Four-Dimensional Quantum Hall Effect in a Two-Dimensional Quasicrystal

Yaacov E. Kraus,[1] Zohar Ringel,[1,2] and Oded Zilberberg[1,3]

[1]*Department of Condensed Matter Physics, Weizmann Institute of Science, Rehovot 76100, Israel*
[2]*Theoretical Physics, Oxford University, 1, Keble Road, Oxford OX1 3NP, United Kingdom*
[3]*Institute for Theoretical Physics, ETH Zurich, 8093 Zürich, Switzerland*

(Received 10 February 2013; published 25 November 2013)

One-dimensional (1D) quasicrystals exhibit physical phenomena associated with the 2D integer quantum Hall effect. Here, we transcend dimensions and show that a previously inaccessible phase of matter—the 4D integer quantum Hall effect—can be incorporated in a 2D quasicrystal. Correspondingly, our 2D model has a quantized charge-pump accommodated by an elaborate edge phenomena with protected level crossings. We propose experiments to observe these 4D phenomena, and generalize our results to a plethora of topologically equivalent quasicrystals. Thus, 2D quasicrystals may pave the way to the experimental study of 4D physics.

DOI: 10.1103/PhysRevLett.111.226401 PACS numbers: 71.23.Ft, 05.30.Rt, 73.43.Nq

The uprising field of topological phases of matter deals with systems of arbitrary dimension [1,2]. In this paradigm, each energy gap of a system is attributed an index, which is robust to continuous deformations. A nontrivial index is usually associated with interesting boundary phenomena, quantized response, and exotic quasiparticles. While nontrivial topological phases appear in any dimension [3,4], the physical manifestations are limited to 1D [5,6], 2D [7,8], and 3D [9].

An example of an intriguing topological phase, which is seemingly out of reach, is the 4D generalization of the 2D integer quantum Hall effect (IQHE). In 2D, a uniform magnetic field creates Landau levels that are characterized by the 1st Chern number (1CN)—the topological index that corresponds to the quantized Hall conductance [10,11]. In 4D, a uniform SU(2) Yang-Mills field results in generalized Landau levels [12,13]. These levels are characterized by the 2nd Chern number (2CN)—a topological index which corresponds to a quantized nonlinear response [13,14]. Both the 2D and 4D IQHEs exhibit a variety of exotic strongly correlated phases when interactions are included [13,15]. Hence, the 4D IQHE, as well as lattice models with nonvanishing 2CNs, constantly attract theoretical attention [14,16], such as the recently found rich metal-insulator phase diagram [17].

The physical properties of quasicrystals (QCs)—nonperiodic structures with long-range order—can oftentimes be derived from periodic models of higher dimensions [18,19]. Using a novel dimensional extension, it was recently shown that 1D QCs exhibit topological properties of the 2D IQHE [20]. The bulk energy spectrum of these 1D QCs is gapped, and each gap is associated with a nontrivial 1CN. This association relies on the fact that the long-range order harbors an additional degree of freedom in the form of a shift of the quasiperiodic order. Accordingly, boundary states traverse the gaps as a function of this shift. This property was observed in photonic QCs, and was utilized for an adiabatic pump of light [20]. Moreover, upon a deformation between QCs with different 1CNs, the expected phase transition was experimentally observed [21]. Generalizations to other 1D symmetry classes, physical implementations, and QCs were discussed [22–25].

In this Letter, we take a major step further, and present a 2D quasiperiodic model that exhibits topological properties of the 4D IQHE. Each gap in its energy spectrum is characterized by a nontrivial 2CN, which implies quantum phase transitions between topologically distinct models. Furthermore, scanning of the shift parameters is accompanied by (i) quantized charge pumping with an underlying 4D symmetry and (ii) gap-traversing edge states with protected level crossings. Generalizations to other models and 2D QCs are discussed. We propose two experiments to measure the 2CN via charge pumping, and, thus, make 4D physics experimentally accessible.

We study a 2D tight-binding model of particles that hop on a square lattice in the presence of a modulated on-site potential

$$H(\phi_x, \phi_y) = \sum_{x,y} \sum_{\sigma=\pm} c^{\dagger}_{x,y,\sigma}[t_x c_{x+1,y,\sigma} + t_y c_{x,y+1,\sigma} + \text{H.c.} + (\lambda_x \cos(\sigma 2\pi b_x x + \phi_x) + \lambda_y \cos(\sigma 2\pi b_y y + \phi_y))c_{x,y,\sigma}]. \quad (1)$$

Here, $\sigma = \pm$ is an internal degree of freedom such as spin-$\frac{1}{2}$, photonic polarization, or atomic orbital, $c_{x,y,\sigma}$ is the single-particle annihilation operator of a particle at site (x, y) in state σ; t_x, t_y are the hopping amplitudes in the x and y directions; and λ_x, λ_y are the amplitudes of the on-site potentials, which are modulated along x and y with modulation frequencies b_x, b_y, respectively [cf. Fig. 1(a)]. Last, the Hamiltonian depends on two shift parameters ϕ_x and ϕ_y. We assume the modulation frequencies b_x and b_y to be irrational, which makes the on-site modulations

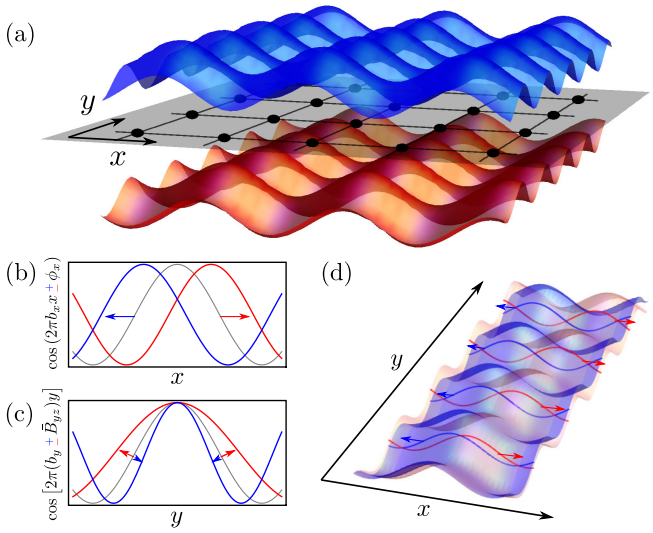

FIG. 1 (color online). (a) An illustration of H [cf. Eq. (1)]: a 2D square lattice with a cosine-modulated on-site potential. The potential is incommensurate with the lattice, and is σ dependent. The state $\sigma = +$ experiences the upper (blue) potential, and $\sigma = -$ experiences the lower (red). For clarity, the potentials are vertically displaced. The dots mark the underlying lattice sites. (b)–(d) A quantized charge pumping along the x direction is achieved by scanning the shift parameters ϕ_x and ϕ_y in the presence of the modulation modifications $\bar{B}_{yz}$ and $\bar{B}_{wy}$, respectively [cf. Eqs. (5) and (7)]. The effects on the potentials of $\sigma = +$ (blue) and $\sigma = -$ (red) is illustrated [the thin (gray) line denotes the unmodified reference potential]: (b) ϕ_x (or, equivalently, ϕ_y) shifts the cosine potentials in opposite directions for opposite σ. (c) $\bar{B}_{yz}$ makes the modulation frequency become σ dependent $b_y + \sigma\bar{B}_{yz}$. (d) $\bar{B}_{wy}$ shifts the cosine potentials in opposite directions, but with an increasing shift along the y direction.

incommensurate with the lattice, and the model becomes quasiperiodic.

The spectrum of H is gapped, and therefore, may exhibit nontrivial topological indices. Conventionally, the only apparent topological index that can be associated with H is the 1CN [3,4]. However, since $H(\phi_x = \phi_y = 0)$ is time-reversal symmetric, its 1CN vanishes, and H is seemingly trivial.

Strikingly, H is attributed a nontrivial 2CN, which, by definition, characterizes 4D systems. In order to obtain this result, let us consider H on a toroidal geometry [26]. We introduce twisted boundary conditions along the x and y directions, parametrized by θ_x and θ_y, respectively. For a given gap and given $\phi_\mu \equiv (\phi_x, \phi_y, \theta_x, \theta_y)$, we denote by $P(\phi_\mu)$ the projection matrix on all the eigenstates of $H(\phi_\mu)$ with energies below this gap. We can now define,

$$\mathcal{C}(\phi_\mu) = \sum_{\alpha\beta\gamma\delta} \frac{\epsilon_{\alpha\beta\gamma\delta}}{-8\pi^2} \mathrm{Tr}\left(P \frac{\partial P}{\partial\phi_\alpha} \frac{\partial}{\partial\phi_\beta} P \frac{\partial P}{\partial\phi_\gamma} \frac{\partial P}{\partial\phi_\delta}\right), \quad (2)$$

where $\epsilon_{\alpha\beta\gamma\delta}$ is the antisymmetric tensor of rank 4.

Formally, the 2CN is defined by $\mathcal{V} = \int d^4\phi_\mu \mathcal{C}(\phi_\mu)$ [27]. By its definition, $\mathcal{V}$ characterizes a 4D family of Hamiltonians composed of all $H(\phi_\mu)$ with all possible values of ϕ_μ; i.e., ϕ_x and ϕ_y act as two additional effective dimensions. The main result of this Letter is that even for a given ϕ_μ, the gaps of $H(\phi_\mu)$ can be associated with a nontrivial integer 2CN,

$$\mathcal{V} = (2\pi)^4 \mathcal{C}(\phi_\mu) \neq 0, \quad (3)$$

in the thermodynamic limit. Below, we justify Eq. (3) by showing that, for our model, $\mathcal{C}(\phi_\mu)$ is essentially independent of ϕ_μ, and thus, the integration over the four parameters is redundant.

Beforehand, we present the physical implications of the nontrivial $\mathcal{V}$. To do so, we apply to H the procedure of dimensional extension that was introduced in Refs. [20,23]. In this procedure, we interpret ϕ_x and ϕ_y as momenta along two fictitious perpendicular coordinates w and z, respectively. Now, the Hamiltonian $H(\phi_x, \phi_y)$ is a single Fourier component of some ancestor 4D Hamiltonian $\mathcal{H}$. By making the inverse Fourier transform, we obtain a Hamiltonian describing spin-$\frac{1}{2}$ particles hopping on a 4D hypercubic lattice

$$\mathcal{H} = \sum_{\mathbf{x},\hat{\mu}} \mathbf{c}_\mathbf{x}^\dagger e^{i2\pi a_{\hat{\mu}}(\mathbf{x})} t_{\hat{\mu}} \mathbf{c}_{\mathbf{x}+\hat{\mu}} + \mathrm{H.c.}, \quad (4)$$

where $\mathbf{c}_\mathbf{x} = (c_{\mathbf{x},+}, c_{\mathbf{x},-})$ annihilates a spin-$\frac{1}{2}$ particle at site $\mathbf{x} = (x, y, z, w)$, $\hat{\mu}$ is summed over the unit vectors $\hat{x}$, $\hat{y}$, $\hat{z}$, and $\hat{w}$, which connect nearest neighbors, and $t_{\hat{\mu}} = (t_x, t_y, \lambda_x/2, \lambda_y/2)$. These particles are coupled to a Yang-Mills gauge field $a_{\hat{\mu}}(\mathbf{x}) = (b_y y\hat{z} + b_x x\hat{w})\sigma_3$. This vector potential describes a spin-polarized uniform SU(2) field. Such a field is known to generate a 4D IQHE with a nontrivial $\mathcal{V}$ [12,13]. Notably, $\mathcal{H}$ is defined on a planar geometry in a Landau gauge, whereas previous analyses treated a spherical geometry in a symmetric gauge.

Similar to the 2D IQHE, $\mathcal{V}$ has a physical manifestation in the form of a response function. Here the response is quantized but nonlinear: $j_\alpha = \mathcal{V}(e^2/h\Phi_0)\epsilon_{\alpha\beta\gamma\delta} B_{\beta\gamma} E_\delta$ [14], where j_α denotes the current density along the α direction, Φ_0 is the flux quantum, E_δ is an electric field along the δ direction, and $B_{\beta\gamma}$ is a magnetic field in the $\beta\gamma$ plane.

A direct observation of this response requires a 4D system. However, we can develop an analogue of Laughlin's pumping, which is manifested in the 2D model. Let us consider the following two cases: $j_x = \mathcal{V}(e^2/h\Phi_0)B_{yz}E_w$ and $j_x = \mathcal{V}(e^2/h\Phi_0)B_{wy}E_z$. Recall that the electric fields can be generated by time-dependent Aharonov-Bohm fluxes, $E_w = (1/caN_w)\partial_t\Phi_w(t)$ and $E_z = (1/caN_z)\partial_t\Phi_z(t)$, where a is the lattice spacing, and N_w and N_z are the number of lattice sites along the w and z directions, respectively. Expressing B_{yz} and B_{wy} in $\mathcal{H}$ in Landau gauge, and performing dimensional

reduction, these fields enter the 2D model, H, through modified on-site terms,

$$\lambda_x \cos[2\pi(\sigma b_x x + \bar{B}_{wy} y) + \phi_x(t)] + \lambda_y \cos[2\pi(\sigma b_y + \bar{B}_{yz}) y + \phi_y(t)], \quad (5)$$

where $\phi_x(t) = (2\pi/N_w\Phi_0)\Phi_w(t)$ and $\phi_y(t) = (2\pi/N_z\Phi_0)\Phi_z(t)$, and $\bar{B}_{wy} = B_{wy}a^2/\Phi_0$ and $\bar{B}_{yz} = B_{yz}a^2/\Phi_0$ denote the corresponding flux quanta per plaquette. Figures 1(b)–1(d) illustrate the effects of these modifications. By fixing the chemical potential within a gap with a given $\mathcal{V}$, an adiabatic scan of ϕ_x or of ϕ_y from 0 to 2π pumps charge along the x direction, such that

$$Q_x = \mathcal{V} e \bar{B}_{yz} N_y, \quad (6a)$$

$$Q_x = \mathcal{V} e \bar{B}_{wy} N_y, \quad (6b)$$

respectively, where N_y is the number of lattice sites along the y direction.

We can now propose experiments that measure $\mathcal{V}$ using Eq. (7). Take a 2D slab of our model, and connect metal leads to the edges of the x coordinate. Let us assume that the chemical potential of both the system and the leads is placed in some gap of H. Then, one should measure the charge-flow during the scan of ϕ_x from 0 to 2π for different values of $\bar{B}_{yz}$ [28]. According to Eq. (6a), we expect that $\mathcal{V} = (1/eL_y)\partial Q_x/\partial \bar{B}_{yz}$. Similarly, according to Eq. (6b) during the scan of ϕ_y while varying $\bar{B}_{wy}$, charge flows and $\mathcal{V} = (1/eL_y)\partial Q_x/\partial \bar{B}_{wy}$. Remarkably, due to the 4D origin of our model, the measured $\mathcal{V}$ would be the same in both experiments. A similar experiment can be conducted in a photonic system [29].

We have just seen that upon a scan of ϕ_x, charge may flow in the x direction. Consequently, for an open geometry, in order to accommodate this charge transfer, edge states must appear and traverse the gaps as a function of ϕ_x. These states appear for infinitesimally small $\bar{B}_{yz}$ and, hence, appear also for $\bar{B}_{yz} = 0$. Figure 2 depicts the numerically obtained energy spectrum of H as a function of ϕ_x, for an open x coordinate, a periodic y coordinate, $t_x = t_y = 1$, $\lambda_x = \lambda_y = 1.8$, $N_x = N_y = 34$, $b_x = (1+\sqrt{5})/2$, and $b_y = 55/34 \approx (1+\sqrt{5})/2$ [26]. The spectrum is invariant with respect to ϕ_y, and is depicted for $\phi_y = 0$. As a function of ϕ_x, the spectrum has flat bands and gap-traversing bands. The flat bands correspond to bulk states, whereas the gap-traversing ones to edge states (see insets). The edge states are divided into four types: $\sigma = +$ and $\sigma = -$ (blue and red), which are localized at either the left or right edge (opposite slopes). These edge states are a signature of the nontrivial $\mathcal{V}$ of our model. They can be measured in a way similar to the experiments performed in 1D photonic QCs [20,29].

Naively, opposite-σ modes that reside on the same edge can be gapped out by introducing σ-mixing terms. However, this is not the case, and the edge modes and their

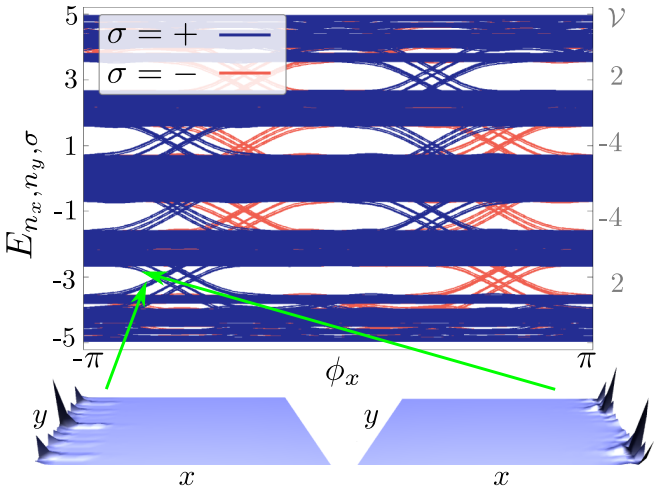

FIG. 2 (color online). The spectrum of H as a function of the shift parameter ϕ_x [cf. Eq. (1)], for an open x coordinate and a periodic y coordinate. The horizontal bands correspond to bulk states. The gap-traversing states with $\sigma = +$ (blue) or $\sigma = -$ (red) are edge states, which are localized at the left or right edges (see insets for typical wave functions). The crossings of edge states are topologically protected. The values of the 2nd Chern number, $\mathcal{V}$, associated with the large gaps are presented.

crossings are topologically protected. In order to establish this protection, we decompose H into its σ and spatial constituents. The Hamiltonian H is a sum of two σ components, where each σ component is subject to two decoupled 1D Harper models along the x and y directions. Both σ components experience the same modulation frequencies, b_x and b_y, but couple to the shift parameters, ϕ_x and ϕ_y, with an opposite sign. Therefore, each eigenstate of $H(\phi_x, \phi_y)$ is a product of eigenstates of the Harper models in the x and y directions and an eigenstate of σ.

Recall that each gap of the Harper model is associated with a nontrivial 1CN, which corresponds to the number of boundary states that traverse the gap as a function of ϕ [10,11,20]. Accordingly, each band of the Harper models in the x and y directions is associated with some σ-dependent 1CN, $\nu_{r_x,\sigma}$ and $\nu_{r_y,\sigma}$, where r_x and r_y denote the corresponding bands, respectively, [30]. In Fig. 2, the bands that traverse the gaps as a function of ϕ_x are composed of products of bulk bands in the y direction and boundary states in the x direction. Notably, due to the opposite coupling of σ to ϕ_x and ϕ_y, $\nu_{r_x,-} = -\nu_{r_x,+}$ and $\nu_{r_y,-} = -\nu_{r_y,+}$. Therefore, the gaps are traversed by the same number of $\sigma = \pm$ bands, but with opposite slopes. Since opposite-σ bands are associated with opposite 1CNs, they cannot be gapped out by σ-mixing terms, even if they cross at some value of ϕ_x. Otherwise, $\nu_{r_y,\sigma}$ would change continuously as a function of ϕ_x between $\nu_{r_y,+}$ and $\nu_{r_y,-}$. The level crossing is, therefore, protected.

The described edge phenomena accounts for the charge pumping described above. When ϕ_x or ϕ_y are scanned,

opposite-σ states, which have opposite 1CNs, flow in opposite directions. In the absence of $\bar{B}_{yz}$ and $\bar{B}_{wy}$, the two charge currents cancel. Applying $\bar{B}_{yz}$ or $\bar{B}_{wy}$ causes a difference between the densities of the σ states, and thus, a net charge is pumped [14,31]. Remarkably, for a spin-$\frac{1}{2}$ realization, our model can serve as a spin pump across the sample, since for recursive scans of ϕ_x, macroscopic spins accumulate at the boundaries, even for vanishing $\bar{B}_{yz}$ and $\bar{B}_{wy}$.

We turn, now, to establish Eq. (3). Let us evoke the definition of the 1CN of a band of the Harper model in the x direction with a given σ, $\nu_{r_x,\sigma} = \int d\phi_x d\theta_x C_{r_x,\sigma}(\phi_x, \theta_x)$, where $C_{r_x,\sigma}(\phi_x, \theta_x) = (1/2\pi i)\mathrm{Tr}(P_{r_x,\sigma}[\partial_{\phi_x} P_{r_x,\sigma}, \partial_{\theta_x} P_{r_x,\sigma}])$, and $P_{r_x,\sigma}(\phi_x, \theta_x)$ is the projection matrix on the eigenstates of the r_xth band [27]. A similar definition applies for $\nu_{r_y,\sigma}$. Let us denote by $\epsilon_n(\phi)$ the eigenenergies of the Harper model. The decomposition of H into x and y constituents makes its energy spectrum a Minkowski sum, $E_{n_x,n_y,\sigma}(\phi_x, \phi_y) = \epsilon_{n_x}(\sigma\phi_x) + \epsilon_{n_y}(\sigma\phi_y)$. Accordingly, the states below each gap of $E_{n_x,n_y,\sigma}$ can be decomposed into a sum over pairs of bands in the 1D spectra, r_x and r_y, such that $\epsilon_{r_x} + \epsilon_{r_y} < \mu$, where μ is the energy in the middle of the gap. Using the fact that the eigenfunctions of H are a product of the 1D eigenfunctions, we obtain [29]

$$\mathcal{V} = \sum_{\sigma=\pm} \sum_{(\epsilon_{r_x}+\epsilon_{r_y}<\mu)} \nu_{r_x,\sigma}\nu_{r_y,\sigma} \neq 0. \tag{7}$$

In a previous work [20], we have shown that, in the thermodynamic limit, $C_{r,\sigma}(\phi, \theta)$ becomes independent of ϕ and θ. Hence, $\nu_{r,\sigma} = (2\pi)^2 C_{r,\sigma}(\phi, \theta)$. This, combined with Eq. (5), immediately implies Eq. (3) [29].

Until now, our analysis used the decomposition of H into σ, x, and y components. In fact, any SU(2) × U(1) gauge transformation in the 4D Hamiltonian $\mathcal{H}$ that respects Landau gauge keeps the system unchanged. After the dimensional reduction to 2D, such a transformation becomes a general local transformation that may mix x, y, and σ, but keeps $\mathcal{V}$ unchanged. More generally, any unitary transformation of the 2D Hamiltonian that does not depend on ϕ_μ keeps $\mathcal{C}(\phi_\mu)$ independent of ϕ_μ. One can also show that the symmetry of H to spin flip is unnecessary [29]. Additionally, in the presence of uncorrelated disorder that does not close the bulk gap, $\mathcal{V}$ remains the same, similar to the 1D case [20].

The predicted 2CN is not limited to a 2D model composed of two Harper models. One can consider (i) placing the cosine modulations in the hopping terms, rather than in the on-site terms (off-diagonal Harper), and (ii) replacing each of the cosine modulations with a Fibonacci-like modulation. Combining (i) and (ii) leads to a well-known 2D QC [32]. In 1D, all these variants were shown to be topologically equivalent to the Harper model, namely, they have the same distribution of 1CNs [23]. Therefore, the gaps in such 2D QC variants will have nontrivial $\mathcal{V}$. Note, also, that similar models that do not depend on σ can have gaps with nontrivial $\mathcal{V}$ with accompanying bulk response and edge phenomena [29].

To conclude, in this Letter, we have presented a novel 2D quasiperiodic model that is associated with the same topological index as the 4D IQHE—the 2nd Chern number. Correspondingly, our model exhibits an elaborate edge phenomena and a quantized charge-pump. We propose experiments in which charge is pumped through the system following modifications of the quasiperiodic modulation. Interestingly, while these modifications differ considerably, they lead to the same pumped charge. This equivalence may seem baffling from a 2D perspective, but follows from the symmetry of the nonlinear response in 4D. Recent progress in controlling and engineering systems, such as optical lattices [33], photonic crystals [34,35], and molecule assembly on metal surfaces [36], makes our 2D model seem experimentally feasible. Moreover, interactions in such systems may lead to fractional quasicrystalline phases which are descendants of the exotic 4D fractional quantum Hall effect [13]. Thus, our model serves as a porthole by which to access 4D physics.

We thank E. Berg and Y. Lahini for fruitful discussions. We acknowledge the Minerva Foundation of the DFG and the US-Israel BSF for financial support. Authors' names appear in alphabetical order.

[1] M. Z. Hasan and C. L. Kane, Rev. Mod. Phys. **82**, 3045 (2010).
[2] X.-L. Qi and S.-C. Zhang, Rev. Mod. Phys. **83**, 1057 (2011).
[3] R. Shinsei, A. P. Schnyder, A. Furusaki, and A. W. W. Ludwig, New J. Phys. **12**, 065010 (2010).
[4] A. Kitaev, AIP Conf. Proc. **1134**, 22 (2009).
[5] V. Mourik, K. Zuo, S. M. Frolov, S. R. Plissard, E. P. A. M. Bakkers, and L. P. Kouwenhoven, Science **336**, 1003 (2012).
[6] A. Das, Y. Ronen, Y. Most, Y. Oreg, M. Heiblum, and H. Shtrikman, Nat. Phys. **8**, 887 (2012).
[7] K. v. Klitzing, G. Dorda, and M. Pepper, Phys. Rev. Lett. **45**, 494 (1980).
[8] M. König, S. Wiedmann, C. Brüne, A. Roth, H. Buhmann, L. W. Molenkamp, X.-L. Qi, and S.-C. Zhang, Science **318**, 766 (2007).
[9] Y. Xia *et al.*, Nat. Phys. **5**, 398 (2009).
[10] D. J. Thouless, M. Kohmoto, M. P. Nightingale, and M. den Nijs, Phys. Rev. Lett. **49**, 405 (1982).
[11] Y. Avron, R. Seiler, and B. Shapiro, Nucl. Phys. **B265**, 364 (1986).
[12] C. Yang, J. Math. Phys. (N.Y.) **19**, 320 (1978).
[13] S.-C. Zhang and J. Hu, Science **294**, 823 (2001).
[14] X.-L. Qi, T. L. Hughes, and S.-C. Zhang, Phys. Rev. B **78**, 195424 (2008).
[15] C. Nayak, S. H. Simon, A. Stern, M. Freedman, and S. Das Sarma, Rev. Mod. Phys. **80**, 1083 (2008).

[16] Y. Li, S. Zhang, and C. Wu, Phys. Rev. Lett. **111**, 186803 (2013).
[17] J. M. Edge, J. Tworzydlo, and C. W. J. Beenakker, Phys. Rev. Lett. **109**, 135701 (2012).
[18] M. Senechal, *Quasicrystals and Geometry* (Cambridge University Press, Cambridge, England, 1996).
[19] A. W. Rodriguez, A. P. McCauley, Y. Avniel, and S. G. Johnson, Phys. Rev. B **77**, 104201 (2008).
[20] Y. E. Kraus, Y. Lahini, Z. Ringel, M. Verbin, and O. Zilberberg, Phys. Rev. Lett. **109**, 106402 (2012).
[21] M. Verbin, O. Zilberberg, Y. E. Kraus, Y. Lahini, and Y. Silberberg, Phys. Rev. Lett. **110**, 076403 (2013).
[22] F. Mei, S.-L. Zhu, Z.-M. Zhang, C. H. Oh, and N. Goldman, Phys. Rev. A **85**, 013638 (2012).
[23] Y. E. Kraus and O. Zilberberg, Phys. Rev. Lett. **109**, 116404 (2012).
[24] Z. Xu, L. Li, and S. Chen, Phys. Rev. Lett. **110**, 215301 (2013).
[25] S. Ganeshan, K. Sun, and S. Das Sarma, Phys. Rev. Lett. **110**, 180403 (2013).
[26] For periodic boundary conditions, b_x and b_y are approximated by rational numbers. The resulting discrepancy vanishes in the thermodynamic limit.
[27] J. E. Avron, L. Sadun, J. Segert, and B. Simon, Commun. Math. Phys. **124**, 595 (1989).
[28] Notably, $\bar{B}_{yz}$ must be sufficiently small to keep the gap open, and should be picked such that $\bar{B}_{yz}N_y$ is approximately an integer.
[29] See Supplemental Material at http://link.aps.org/supplemental/10.1103/PhysRevLett.111.226401 for additional details on: proposed setup for a photonic experiment; factorization of the 2CN; classification beyong the σ-symmetric case; and a spinless model with a nontrivial 2CN.
[30] The spectrum of the quasiperiodic Harper model is fractal. Its energy bands are defined by progressively taking rational approximants of b. The 1CN associated with a band of an approximant as a function of ϕ_y remains the same in the irrational limit even for a given ϕ_y. In our model, the approximants must be sufficiently good such that Harper bands within a gap are narrower than the gap they cross. This way we can also associate each band with its mean energy.
[31] R. Roy, arXiv:1104.1979.
[32] S. Even-Dar Mandel and R. Lifshitz, Philos. Mag. **88**, 2261 (2008).
[33] M. Atala, M. Aidelsburger, J. T. Barreiro, D. Abanin, T. Kitagawa, E. Demler, and I. Bloch, Nat. Phys., doi: 10.1038/nphys2790 (2013).
[34] M. Rechtsman, J. Zeuner, Y. Plotnik, Y. Lumer, S. Nolte, M. Segev, and A. Szameit, Nature (London) **496**, 196 (2013).
[35] M. Hafezi, S. Mittal, J. Fan, A. Migdall, and J. M. Taylor, Nat. Photonics, doi: 10.1038/nphoton.2013.274 (2013).
[36] K. K. Gomes, W. Mar, W. Ko, F. Guinea, and H. C. Manoharan, Nature (London) **483**, 306 (2012).